Mice Lacking α/β Subunits of GlcNAc-1-Phosphotransferase Exhibit Growth Retardation, Retinal Degeneration, and Secretory Cell Lesions

Claire M. Gelfman,[1] Peter Vogel,[2] Tawfik M. Issa,[1] C. Alexander Turner,[3] Wang-Sik Lee,[4] Stuart Kornfeld,[4] and Dennis S. Rice[1]

Purpose. Mucolipidosis II and III (ML II; ML III) are lysosomal storage diseases characterized by a deficiency in GlcNAc-1-phosphotransferase. Patients with ML III have retinal disease, but in cases of the more clinically severe ML II, human ophthalmic studies are limited. In this study, retinal function and overall disease were assessed in mice lacking *GNPTAB*, the gene mutated in patients with ML II.

Methods. Mice deficient in *GNPTAB* were generated from Omnibank, a sequence-tagged gene-trap library of >270,000 mouse embryonic stem cell clones as part of a large-scale effort to knock out, phenotypically screen, and thereby validate pharmaceutically tractable genes for drug development. Routine diagnostics, expression analysis, histopathology, and ERG analyses were performed on mice lacking *GNPTAB*. In addition, measurements of serum lysosomal enzymes were performed.

Results. Severe retinal degeneration was observed in mice deficient in *GNPTAB*. Heterozygous mice were phenotypically normal and in situ hybridization showed expression across the neural retina. Compared to wild-type mice, the *GNPTAB* homozygous mice were smaller, had elevated levels of serum lysosomal enzymes, exhibited cartilage defects, and had cytoplasmic alterations in secretory cells of several exocrine glands.

Conclusions. Mice deficient in *GNPTAB* exhibited severe retinal degeneration. Additional features observed in patients with ML II, a lysosomal storage disease, are also present in these mice. Understanding underlying mechanisms of this gene in the eye will increase its therapeutic potential for the treatment of retinal diseases. (*Invest Ophthalmol Vis Sci.* 2007;48: 5221–5228) DOI:10.1167/iovs.07-0452

Mucolipidosis II and III (ML II; ML III) are autosomal recessive lysosomal storage diseases characterized by a deficiency of UDP-GlcNAc:Lysosomal enzyme *N*-acetylglucosamine-1-phosphotransferase (abbreviated GlcNAc-1-phosphotransferase). This enzyme catalyzes the first step in the synthesis of the mannose 6-phosphate recognition marker that is necessary for efficient intracellular targeting of newly synthesized lysosomal hydrolases to the lysosome in many cell types.[1] GlcNAc-1-phosphotransferase is a hexameric enzyme complex consisting of three different subunits: α_2, β_2, and γ_2.[2] The γ-subunit, which is encoded by the *GNPTG* gene, facilitates the recognition of protein determinants on lysosomal enzymes. Mutations in *GNPTG* have been found in patients with ML III, the milder of the two disorders.[3–7] The α and β subunits contain the catalytic activity and are encoded by a single gene, *GNPTAB*.[8] Mutations in *GNPTAB* that result in a complete loss of enzymatic activity are found in patients with MLII.[3–7,9] Mucolipidosis II is very progressive, and patients rarely survive past the first decade of life.[1]

An animal model of human ML II was reported in a colony of domestic short hair cats that displayed several clinical and radiographic features similar to those in the human disease.[10] Kittens had diffuse retinal degeneration leading to blindness by 4 months of age. In addition, triple-knockout mice deficient in insulin-like growth factor 2 (IGF-II) and the two Man-6-P receptors (CI-MPR and CD-MPR) displayed features resembling those of ML II, including dwarfism and facial dysmorphism.[11,12] However, this model is complicated since the loss of IGF-II alone leads to growth retardation, and the CI-MPR has been shown to have functions in addition to mediating lysosomal enzyme trafficking. In this study, we report the phenotypic consequences of mice lacking *GNPTAB*.

Materials and Methods

Generation of *GNPTAB*$^{-/-}$ Mutant ES Cells and Mice

The generation of the OmniBank gene trap library has been described.[13,14] *GNPTAB* mutant mice were generated by microinjection of embryonic stem (ES) cell clones into host blastocysts using standard methods.[15] The precise genomic insertion site of the retroviral gene-trapping vector in the *GNPTAB* gene was determined by inverse genomic PCR as described.[16] Mice used in this study were of mixed genetic background (129/SvEv^{Brd} and C57BL/6J). All studies were performed in accordance with the ARVO Statement for the Use of Animals in Ophthalmic and Vision Research.

Genotyping of OmniBank Mice

Oligonucleotide primers (LTR2, 5′-AAATGGCGTTACTTAAGCTAGCTTGC-3′, A 5′-*ACCAAGTGCTTATCTCAGAGTAGG*-3′ and B 5′-*AAGATGGCGAAGACTGTACTAGACT*-3′) were used in two separate reactions to amplify corresponding wild-type and mutant *GNPTAB* alleles. Diluted mouse tail lysates containing approximately 20 ng of genomic DNA were used as a template for PCR in a 50-μL reaction volume containing 3.5 mM $MgCl_2$. The PCRs were run under touchdown conditions: 94°C for 15 seconds, 65°C for 30 seconds (then decrease 1°C per cycle), 72°C, 40 seconds, 10 cycles; and 94°C for 15 seconds, 55°C for 30 seconds, 72°C, 40 seconds, 30 cycles. Amplified products were separated on 3% agarose gels.

From the Departments of [1]Ophthalmology, [2]Pathology, and [3]Clinical Development, Lexicon Pharmaceuticals, Inc., The Woodlands, Texas; and the [4]Department of Internal Medicine, Washington University School of Medicine, St. Louis, Missouri.

Presented at the annual meeting of the Association for Research in Vision and Ophthalmology, Fort Lauderdale, Florida, May 2006.

Supported by National Cancer Institute Grant CA08759 (SK).

Submitted for publication April 17, 2007; revised June 12, 2007; accepted September 5, 2007.

Disclosure: **C.M. Gelfman**, Lexicon Pharmaceuticals, Inc. (E); **P. Vogel**, Lexicon Pharmaceuticals, Inc. (E); **T.M. Issa**, Lexicon Pharmaceuticals, Inc. (E); **C.A. Turner**, Lexicon Pharmaceuticals, Inc. (E); **W.-S. Lee**, None; **S. Kornfeld**, None; **D.S. Rice**, Lexicon Pharmaceuticals, Inc. (E)

The publication costs of this article were defrayed in part by page charge payment. This article must therefore be marked "*advertisement*" in accordance with 18 U.S.C. §1734 solely to indicate this fact.

Corresponding author: Claire M. Gelfman, Department of Ophthalmology, Lexicon Pharmaceuticals, Inc., 8800 Technology Forest Place, The Woodlands, TX 77381; cgelfman@lexpharma.com.

GNPTAB RT-PCR

RNA was extracted from whole eyes using a bead homogenizer and extraction reagent (RNAzol; Ambion, Austin, TX), according to the manufacturer's instructions. Reverse transcription was performed with reverse transcriptase (SuperScript II; Invitrogen; Carlsbad, CA) and random hexamer primers, according to the manufacturer's instructions. PCR amplification (95°C, 30 seconds; 59°C, 45 seconds; and 70°C, 60 seconds) was performed for 35 cycles using primers complementary to exons 1 and 2 of the *GNPTAB* gene, flanking the insertion site of the vector (Primer C: 5′-TTGT CACCATCGTCTCGGCTTT-3′, primer D: 5′-CAGAACAAGCATGGGCACC TTAATG-3′). Control primers to the mouse β-actin gene (accession number M12481) were: 5′-GGCTGGCCGGGACCTGACGGACTACCTCAT-3′ and 5′-GCCTAGA AGCACTTGC GGTGCACGATGGAG-3′. *GNPTAB* RT-PCR products were verified by sequencing.

ERG and Fundus Photography

Electroretinograms (ERGs) were recorded from wild-type ($n = 2$) and homozygous ($n = 2$) mice at 5 months of age. All procedures were performed under dim red light (>650 nm). ERGs from both eyes were recorded simultaneously by an electrodiagnostic system (UTAS-E 3000 Visual Electrodiagnostic System; LKC Technologies, Gaithersburg, MD). The mice were deeply anesthetized with (per milliliter) ketamine (7.5 mg), xylazine (0.38 mg), and acepromazine (0.074 mg), delivered at 10 mL/kg body weight. After an overnight dark-adaptation period, the pupil was dilated with 0.1% atropine (Alcon Laboratories Inc., Fort Worth, TX), and 0.5% proparacaine (Alcon) was applied for topical anesthesia. Gold electrodes were placed on the corneal surface with a drop of methylcellulose. A reference electrode was placed SC on the head and a ground electrode was placed in the right hind leg. The animals were placed in a Ganzfeld illumination dome. Full-field scotopic ERGs of both eyes were elicited simultaneously with 10-μs light flashes. Routinely, five recordings per flash intensity were averaged. Mixed rod–cone (scotopic) driven responses to light flashes were recorded, with the intervals between flashes increasing from 10 seconds to 30 seconds with increasing flash intensity range (0.0094–40.41 cd-s/mm^2). Fundus photography was performed using methods described previously.[17]

Histology and Pathology

Histopathology was conducted on mice at 1, 2, 3, and 10 months of age. The mice were euthanatized by CO_2 asphyxiation, and the eyes were removed and placed in Davidson's fixative (Poly Scientific, Bay Shore, NY) overnight at room temperature. The following morning, the eyes were embedded in paraffin, cut at a thickness of 4 μm, and stained with hematoxylin and eosin (H&E). TUNEL staining (DeadEnd Fluorometric TUNEL System; Promega, Madison, WI) was performed on Davidson's-fixed, paraffin-embedded tissues. For pathology, tissues were collected from knockout mice and age-matched normal control mice and were immersion fixed in 10% neutral-buffered formalin. All tissues were embedded in paraffin, sectioned at 4 μm, mounted on positively charged glass slides (Superfrost Plus; Fisher Scientific, Pittsburgh, PA), and stained with H&E for histopathologic examination.

Cathepsin D Immunoblot Analysis

Whole-eye lysates from 5-week-old wild-type, heterozygous, and homozygous mice were prepared by homogenization of snap-frozen tissue in ice-cold RIPA buffer containing protease and phosphatase inhibitors. Lysates were pooled from six eyes (three mice) from each genotype and cleared by centrifugation at 14,000 rpm for 10 minutes, and total protein was quantified using the BCA protein assay (Pierce, Rockford, IL). Aliquots of protein (25 μg) were denatured in a buffer containing 5% SDS and 10% β-mercaptoethanol by boiling for 10 minutes and incubated for 5 hours with either 5000 units of endoglycosidase H (Endo H; New England BioLabs, Ipswich, MA) in 50 mM citrate buffer (pH 5.5; final volume, 40 μL) or 1000 units of peptide N-Glycosidase F (PNGase F; New England BioLabs) in 50 mM Na-phosphate buffer (pH 7.5; final volume, 40 μL), respectively. The proteins were resolved on a 10% SDS polyacrylamide gel, transferred to nitrocellulose membrane (Protran BA 83; Whatman Schleicher & Schuell, Keene, NH) and blocked with TBS-Tween plus 5% nonfat dry milk (blocking buffer) overnight at 4°C. The blot was then incubated for 1 hour at room temperature with rabbit polyclonal cathepsin D antibody (gift of Walter Gregory, Washington University, St. Louis, MO) at 1:2000 dilution in 1% milk TBS-Tween buffer. After three 10-minute washes in TBS-Tween buffer, the membrane was incubated for 1 hour at room temperature with HRP-conjugated rabbit IgG (GE Healthcare, NA934V: 1:2000 in 1% milk TBS-Tween buffer). After three additional 10-minute washes in TBS-Tween, the blots were analyzed by chemiluminescence (ECL-Detection System; GE Healthcare, Piscataway, NJ).

In Situ Hybridization

The method of in situ hybridization analysis was performed as described elsewhere[18] on 16-μm-thick cryosections of eyes taken from 11-month-old wild-type and homozygous mice. A *GNPTAB*-specific cDNA (nucleotides 1221-1605 of accession number AK173132) was generated by PCR with primers that incorporate the T7 RNA polymerase promoter sequence into the PCR amplicon. This DNA template was used for in vitro transcription reaction with 80 μCi of α-^{33}P-UTP (NEN Life Science Products, Boston, MA). After hybridization at 60°C for 16 hours, sections were treated with RNase and washed in SSC buffer. Slides were dehydrated in a graded ethanol series and exposed to a 50% solution of autoradiographic emulsion type NTB2 (Eastman Kodak Company, Rochester, NY) for 3 to 6 days. Slides were developed according to standard protocols[19] and dehydrated, and coverslips were applied (Permount; Fisher Scientific, Pittsburgh, PA). Digital images were acquired (ORCA II; Hamamatsu, Hamamatsu City, Japan) with a cooled charge-coupled device (CCD) camera mounted on a (BX60; Olympus, Lake Success, NY) microscope equipped with dark-field optics.

Lysosomal Enzyme Assays

Serum lysosomal enzyme activities were measured in wild-type ($n = 7$) and homozygous ($n = 5$) mice ranging in age from 4 to 5 months. Measurements from eye lysates were taken from pooled lysates prepared from eyes of three (5-week-old) mice from each genotype. Acid hydrolase assays were performed as previously described with minor modifications.[20] Activities of β-hexosaminidase and β-galactosidase were assayed with 5 mM 4-methylumbelliferyl(MU)-*N*-acetyl-β-D-glucosaminide (Sigma-Aldrich, St. Louis, MO) and 5 mM 4-MU-β-D-galactopyranoside (Calbiochem, San Diego, CA), respectively, in 50 mM citrate buffer containing 0.5% Triton X-100 (pH 4.5). The activity of β-glucuronidase was assayed with 5 mM 4-MU-β-D-glucuronide (Calbiochem) in 0.1 M Na-acetate buffer containing 0.5% Triton X-100 (pH 4.6). The activity of β-mannosidase was assayed with 5 mM 4-MU-β-D-mannopyranoside (Sigma-Aldrich) in 50 mM Na-citrate buffer containing 0.5% Triton X-100 (pH 5.0). The activity of α-mannosidase was assayed with 5 mM 4-MU-α-D-mannopyranoside (Sigma-Aldrich) in 50 mM Na-citrate buffer containing 0.5% Triton X-100 (pH 4.0).

Results

Generation of Mice with Mutant *GNPTAB* Genes

Mouse ES cells carrying a mutation in the GlcNAc-1-phosphotransferase *GNPTAB* gene (accession number, AK173132) were obtained from OmniBank, a library of gene-trapped ES cell clones identified by a corresponding OmniBank sequence tag (OST).[13,14] The ES cell clone corresponding to OST 97730, matching the mouse *GNPTAB* sequence, was thawed and expanded. Inverse genomic PCR[16] analysis of DNA from this clone confirmed insertion of the gene trapping retroviral vector in intron 1 of the *GNPTAB* gene located on mouse chro-

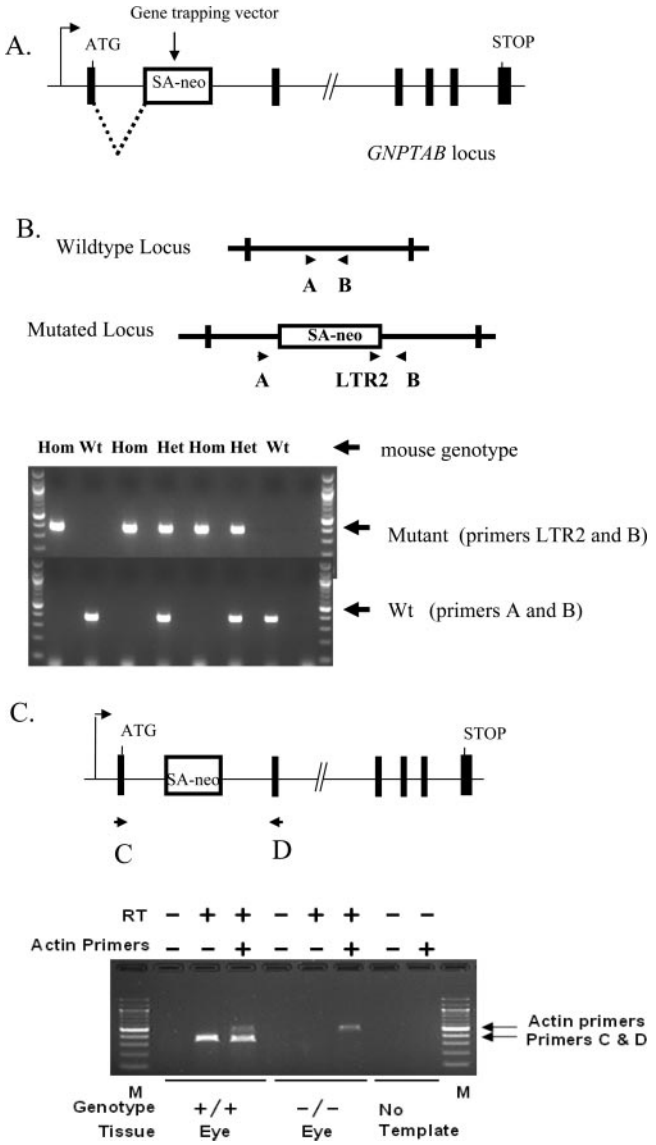

FIGURE 1. (**A**) Gene trap mutation of the *GNPTAB* gene. SA, splice acceptor sequence. Neo, neomycin resistance gene. (**B**) Genotyping strategy. Primers A and B flank the genomic insertion site in intron 1 and amplify a product for the wild-type allele. The LTR2 primer, complementary to the gene-trapping vector, and primer B amplify the mutated allele. (**C**) *GNPTAB* RT-PCR. Primers C and D are complementary to *GNPTAB* exons 1 and 2 flanking the insertion site of the gene-trapping vector. RT-PCR using primers C and D revealed an absence of endogenous message in the eye of homozygous animals. RT, reverse transcription.

mosome 10 (Fig. 1A). This insertion disrupts the full-length *GNPTAB* transcript. ES cells containing OST 97730 were used to generate mice heterozygous for the *GNPTAB* mutation by standard methods.[15] Genotyping of mice was performed by using wild-type and mutant-specific PCR strategies on genomic DNA (Fig. 1B). Mating between *GNPTAB* heterozygous mice gave rise to the expected Mendelian ratios of wild-type, heterozygous, and homozygous animals. This result is similar to that reported for the ML II cats, but differs from the triple knock-out mouse model in which some triply deficient mice died perinatally.[11] To confirm the disruption of *GNPTAB* transcription by the gene trapping vector, we performed reverse transcription-PCR (RT-PCR) with primers complementary to *GNPTAB* exons 1 and 2, flanking the integration site of the vector. Wild-type *GNPTAB* transcript was not detected in tissues of *GNPTAB*$^{-/-}$ mice (Fig. 1C).

Patients with ML II or -III have greatly elevated levels of lysosomal enzymes in their sera because of the inability to synthesize the Man-6-P recognition marker that is essential for proper targeting of these enzymes to lysosomes.[1] This trafficking defect results in hypersecretion of the enzymes into the blood. Table 1 shows that compared with wild-type mice, the *GNPTAB*$^{-/-}$ mice exhibit 6.7- to 13.9-fold increased levels of lysosomal enzymes, as would be expected if GlcNAc-1-phosphotransferase activity were defective in the homozygous mice and consistent with observations in humans.

Pathology

A comprehensive phenotypic analysis was performed on wild-type, heterozygous, and homozygous animals.[21] At all ages examined, heterozygous mice were comparable to their wild-type counterparts. The *GNPTAB*$^{-/-}$ mice were easily discernible from their control littermates by their small size. Mean body weight and length (Figs. 2A, 2B) were significantly reduced in the homozygous animals, along with a reduction in total tissue mass and lean body mass (data not shown). Consistent with their small size, the homozygous mice exhibited a decreased mean femoral midshaft cortical thickness (data not shown). The osteoblasts and osteoclasts appeared normal by light microscopy. However, in mice lacking *GNPTAB*, tracheal chondrocytes were markedly hypertrophic and completely filled their enlarged lacunae (Figs. 2C, 2D). The cytoplasm of the chondrocytes was distended by scanty amounts of finely granular amphophilic material and abundant microvacuoles. In contrast, wild-type chondrocytes generally had minimal eosinophilic cytoplasm containing a single large, clear vacuole and usually only partially filled the lacunar space.

One of the characteristic features of ML II is the accumulation of cytoplasmic inclusions in fibroblasts from affected patients.[1,22,23] The contents of the inclusions have not been well characterized. Inclusion bodies and other lesions were absent in fibrocytes and fibroblasts in all tissues examined from mice deficient in *GNPTAB*. Instead, analysis of tissue from *GNPTAB*$^{-/-}$ mice revealed notable changes in secretory cells of several exocrine glands, including the pancreas, parotid salivary glands, submandibular salivary glands, Steno (lateral nasal) glands, bulbourethral glands, gastric glands, and pancreatic acinar cells (Figs. 3A, 3B). The pancreatic lesion was characterized by disorganization of tissue architecture shown by the marked diffuse, cytoplasmic alteration and cytomegaly of the acinar cells. Similarly, in the parotid salivary glands, acinar cells were distended by large vacuoles that frequently

TABLE 1. Lysosomal Enzyme Activities in Serum of Wild-Type and *GNPTAB*$^{-/-}$ Mice

	Activity (nanomoles/h/mL)*		
Enzyme	GNPTAB Wild-Type (+/+) (n = 7)	GNPTAB Homozygous (−/−) (n = 5)	Fold Increase
β-Hexosaminidase	311 ± 114	2087 ± 318	6.7
β-Mannosidase	156 ± 33	1464 ± 211	9.4
β-Galactosidase	20 ± 8	277 ± 65	13.9
β-Glucuronidase	34 ± 14	382 ± 92	11.2

*Data are the mean ± SD.

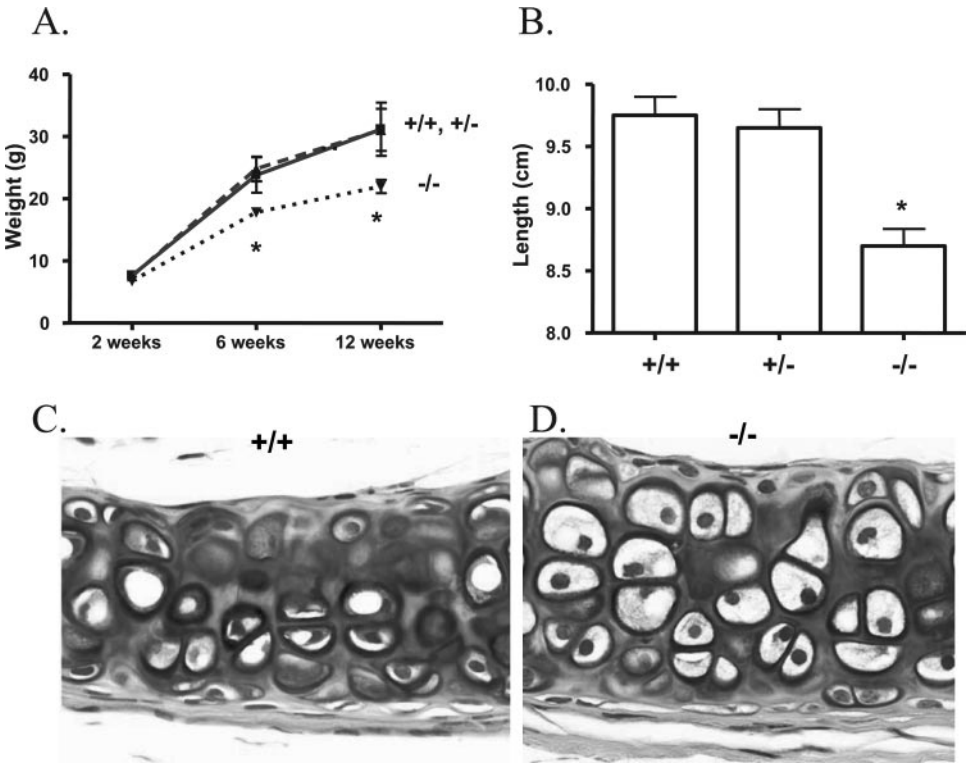

FIGURE 2. Growth retardation and connective tissue cell defects in mice lacking *GNPTAB*. (**A**) Body weight in grams of wild-type (+/+; $n = 3$), heterozygous (+/−; $n = 3$), and homozygous (−/−; $n = 7$) mice at 2, 6, and 12 weeks of age (*$P < 0.05$; one-way ANOVA; Dunnett multiple comparison test). (**B**) Naso-anal length (cm) of wild-type (+/+; $n = 2$), heterozygous (+/−; $n = 2$), and homozygous (−/−; $n = 6$) taken at 14 to 16 weeks of age. (*$P < 0.05$; one-way ANOVA, Bonferroni multiple comparison test). Light microscopy of representative sections of hematoxylin and eosin-stained tracheal cartilage from wild-type (**C**) and homozygous (**D**) mice. In normal cartilage, clear lacunar space typically surrounds chondrocytes that shrink during fixation. Chondrocytes tend to have a pale eosinophilic cytoplasm that frequently contains a single large, clear vacuole. (**D**) In homozygous mice, the cytoplasm of hypertrophic chondrocytes is more basophilic and is distended by microvacuoles containing scanty amounts of finely granular amphophilic material. There is less fixation-related shrinkage of chondrocytes, which fills the enlarged lacunae.

contained small amounts of ill-defined amphophilic-staining tissue (Figs. 3C, 3D). The acinar cells of the submandibular salivary gland were also distended, but in these cells the cytoplasm contained myriad microvacuoles and inclusions, giving a foamy appearance to the cytoplasm. Widespread vacuolization was present in the bulbourethral glands and in the dorsal portion of the Steno glands. The ventral portion of the Steno glands was minimally affected.

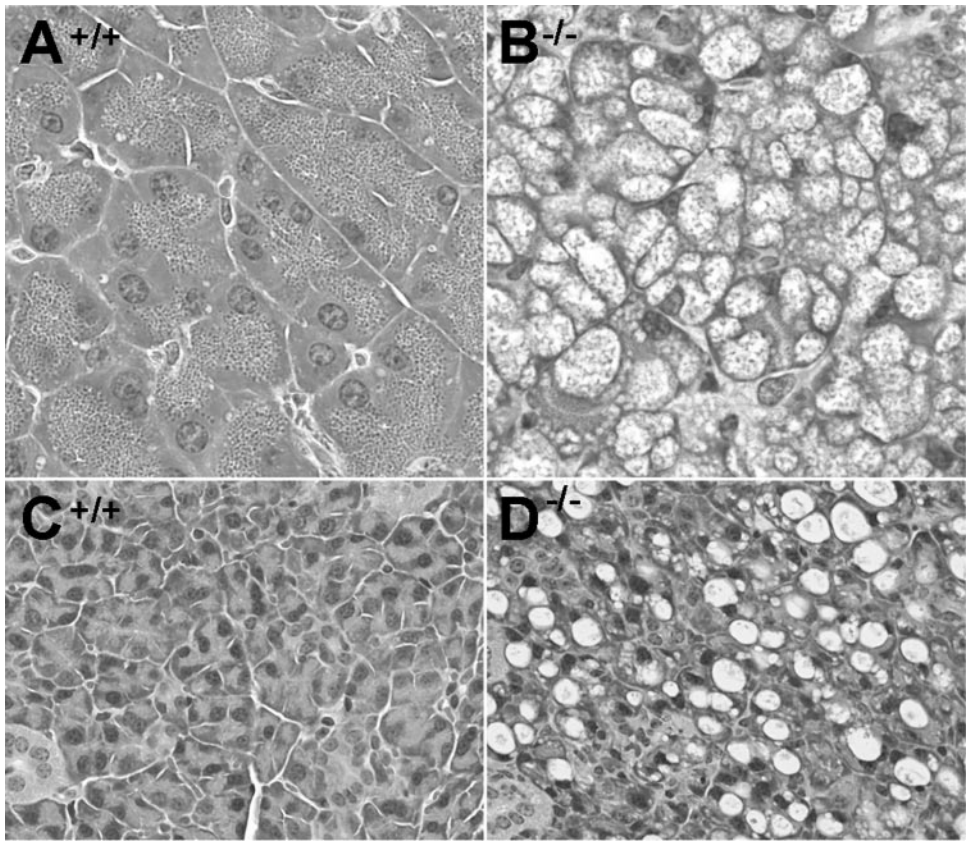

FIGURE 3. Light microscopy of representative sections of H&E-stained pancreas and parotid salivary gland from wild-type (+/+) (**A**, **C**) and homozygous (−/−) (**B**, **D**) mice. (**A**) In the pyramidal acinar cells of normal exocrine pancreas, the basal nucleus is surrounded by cytoplasm, whereas the secretory acidophilic zymogen granules are concentrated in the apical region. (**B**) In homozygous (−/−) mice, there is a marked diffuse, disorganization of the exocrine pancreas characterized by tightly packed clusters cells of variable size that are distended by large vacuoles containing amphophilic granular material (inclusions). The ballooning inclusions are typically located at the base and perinuclear areas of cells, and they efface the zone of basophilia normally present in these areas. Note the marked decrease in size and number of zymogen granules at the apex of acinar cells. (**C**) In the normal parotid gland, the small pyramidal acinar cells also have basal nuclei surrounded by basophilic cytoplasm, with secretory granules concentrated in apical regions of the cells. (**D**) In contrast, the disorganized parotid acinar cells in homozygous (−/−) mice are distended by large vacuoles containing small amounts of faintly stained fibrillogranular material. Original magnification: (**A**, **B**) ×600; (**C**, **D**) ×200.

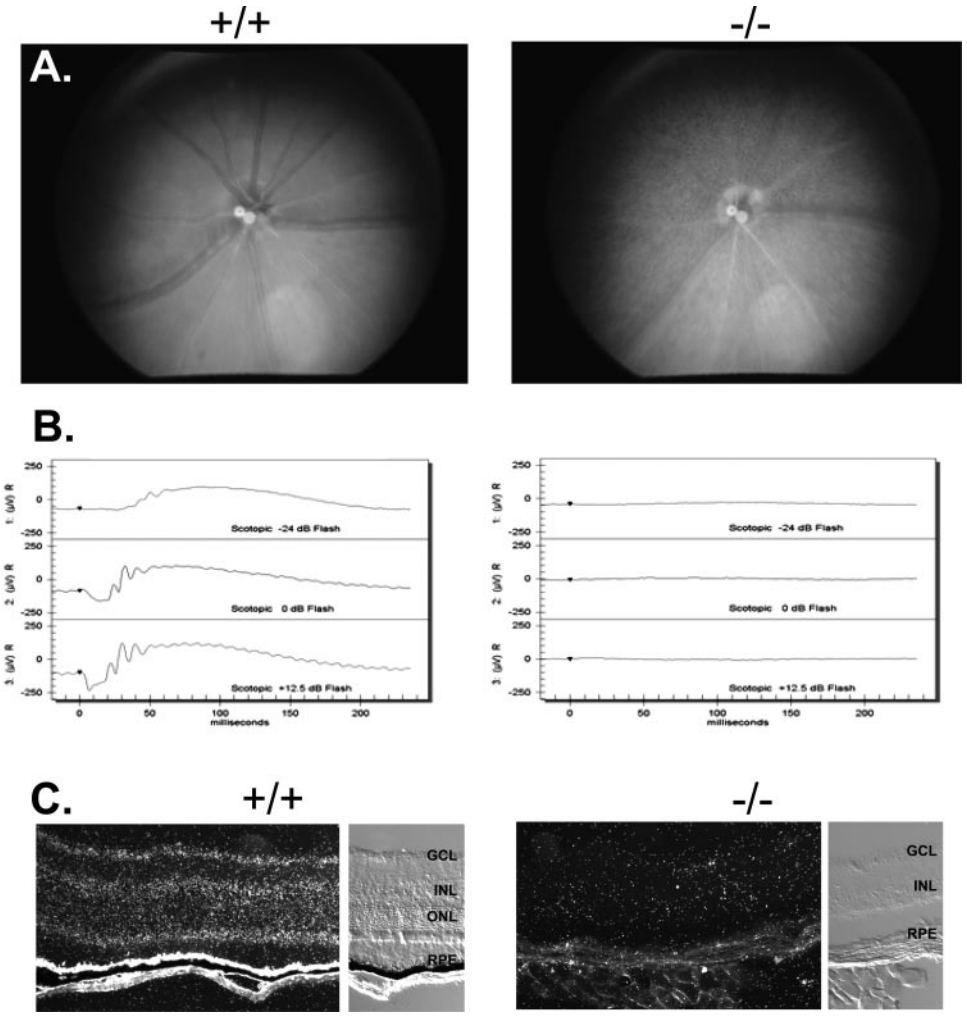

FIGURE 4. (**A**) Fundus photography of *GNPTAB* wild-type (+/+) and homozygous (−/−) mice at 14 weeks of age. The posterior eye in wild-type mice appeared normal, whereas retinal depigmentation was observed in mice lacking *GNPTAB*. (**B**) Electroretinography was performed on wild-type ($n = 2$) and homozygous ($n = 2$) mice at 5 months of age. A representative ERG from each genotype is shown. Mixed rod–cone driven responses to light flashes were measured in wild-type and homozygous mice. Mice lacking *GNPTAB* failed to show an ERG response. (**C**) Expression of *GNPTAB* in the adult eye. Dark-field micrograph of whole-eye sections from 11-month-old wild-type and homozygous mice incubated with an antisense riboprobe specific for *GNPTAB*. The companion light micrograph taken with differential interference contrast (DIC) optics is shown to the right of each dark-field micrograph. High levels of *GNPTAB* expression were detected in the ONL, INL, and GCL of the wild-type animal. No hybridization was obtained with the same probe on a whole-eye section from the homozygous animal.

Retinal Degeneration in *GNPTAB* Homozygous Knock-Out Mice

Patients with ML III have retinal disease,[24] but in cases of the more clinically severe ML II, human ophthalmic studies are not comprehensive. Funduscopic examination of *GNPTAB*-knockout mice at 15 weeks of age showed numerous retinal depigmentation spots with attenuated retinal vessels, indicating retinal degeneration in these mutants (Fig. 4A). The fundus in heterozygous animals was normal (data not shown). All photoreceptor function in $GNPTAB^{-/-}$ mice was ablated by 5 months of age as measured by electroretinography (ERG; Fig. 4B). This ocular phenotype in $GNPTAB^{-/-}$ mice prompted us to examine the expression pattern of this gene in the eye. In situ hybridization revealed expression of *GNPTAB* mRNA throughout the entire neural retina in wild-type animals (Fig. 4C). No signal was observed in the $GNPTAB^{-/-}$ eye sections, confirming the specificity of the riboprobe.

Histopathological analysis was performed to evaluate the timing and extent of retinal degeneration. At 1 month of age, the heterozygous (Fig. 5A) and homozygous retinas (Fig. 5B) were indistinguishable at the level of routine histologic sections. Three cellular layers including the outer and inner nuclear layer (ONL and INL, respectively) and the retinal ganglion cell layer (GCL) were comparable among genotypes. These results indicate that retinal development occurs normally in the absence of *GNPTAB*. Although overall retinal anatomy appeared preserved at this age, an increase in TUNEL-positive cells in the photoreceptor layer was observed in mice lacking *GNPTAB* (Fig. 5B, arrows). Photoreceptor degeneration progressed slowly, as demonstrated in histologic sections obtained from homozygous animals at 2 months of age (Fig. 5C). One month later, severe photoreceptor degeneration was observed in the $GNPTAB^{-/-}$ retina (Fig. 5D). At 3 months of age in wild-type mice, the ONL contains 10 to 12 rows of photoreceptors. In mice lacking *GNPTAB*, photoreceptors were reduced to one to three rows of cells. The underlying retinal pigment epithelium (RPE) also exhibited hypertrophy and dividing RPE cells were observed at this age (Fig. 5D, arrow). The remaining cellular layers appeared histologically normal in the $GNPTAB^{-/-}$ animals. At 10 months of age, photoreceptor degeneration was complete and geographic atrophy of the RPE was observed (Fig. 5E, arrow). Retinas obtained from heterozygous animals at 18 months of age appeared histologically normal (Fig. 5F), confirming the recessive nature of this mutation. These results suggest *GNPTAB* is required for the maintenance of normal retinal anatomy and physiology.

Despite the profound retinal degeneration observed in the mice lacking *GNPTAB*, the activity of five acid hydrolases in whole-eye extracts was not diminished compared with the wild-type levels (Table 2). We next examined cathepsin D, one of the critical lysosomal enzymes involved in photoreceptor outer segment processing in the RPE. Lack of this protease in mice results in retinal degeneration with marked apoptosis of photoreceptors.[25] Whole-eye lysates from wild-type, heterozygous, and homozygous mice were subjected to immunoblot analysis with anti-cathepsin D antibodies. The major cathepsin

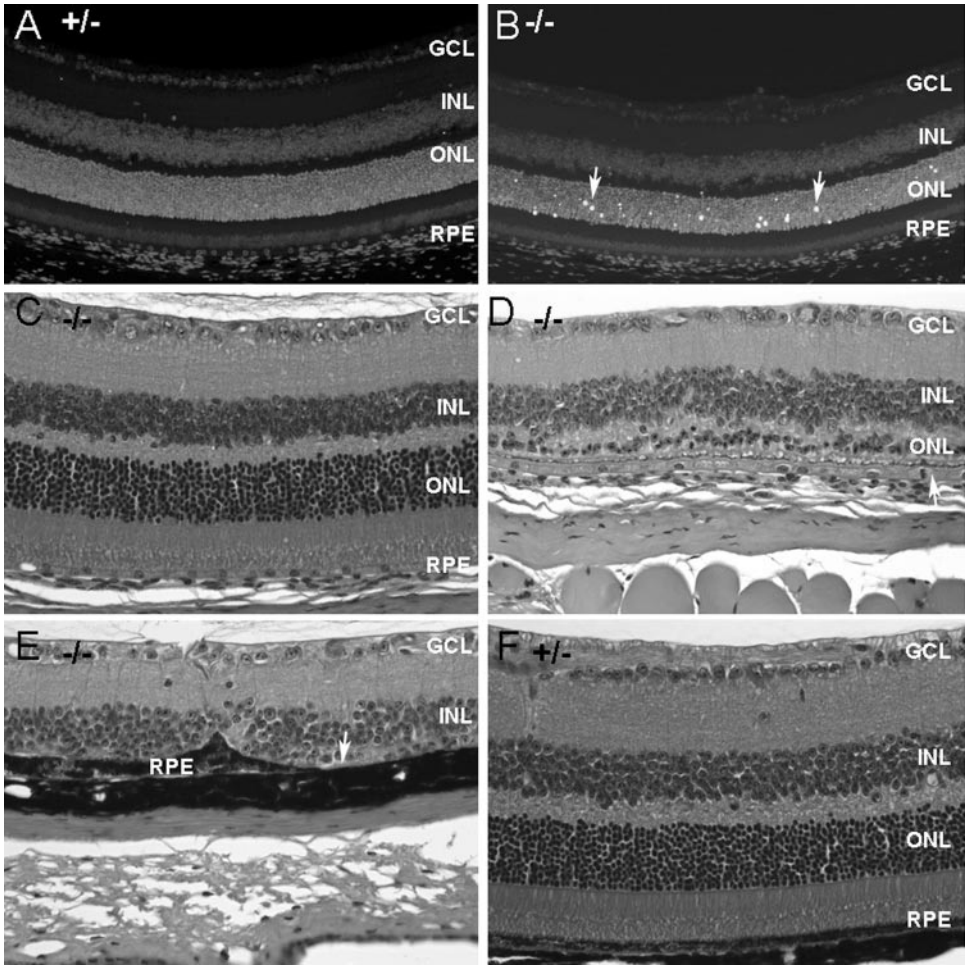

FIGURE 5. Histopathology and TUNEL analysis of heterozygous (+/−) and homozygous (−/−) mice. TUNEL analysis of (+/−) (**A**) and (−/−) (**B**) mice at 1 month of age. Sections were counterstained with DAPI to visualize nuclei. Histopathology of 2-month-old (−/−) (**C**), 3-month-old (−/−) (**D**), 10-month-old (−/−) (**E**), and 18-month-old (+/−) mice (**F**). At least two mice from each time point were analyzed, and representative images are shown. ONL, outer nuclear layer; inner nuclear layer, INL; ganglion cell layer, GCL. Original magnification: (**A**, **B**) ×200; (**C–F**) ×600.

D isoform detected in both the wild-type and the heterozygous lysates was approximately 43 kDa, indicative of the mature species (Fig. 6). The lysate of the *GNPTAB*$^{-/-}$ mice showed this band as well as an additional slower migrating band. To determine whether the cathepsin D molecules in the three lysates differed in the nature of their two N-linked glycans, aliquots were treated with Endo H or PNGase before electrophoresis. Endo H selectively cleaves high-mannose–type N-linked glycans whereas PNGase cleaves both high mannose and complex-type species. As shown in Figure 6, Endo H treatment caused essentially all the cathepsin D from wild-type and heterozygous eye samples to migrate faster on the gels and PNGase increased the migration only slightly more. This result indicates that most of the cathepsin D in these lysates contains two high-mannose units, whereas a minority of the molecules contains one high-mannose unit and one complex-type unit. In contrast, the upper band of the cathepsin D from the *GNPTAB*$^{-/-}$ lysate was resistant to Endo H, whereas approximately half of the lower band migrated faster after incubation with this enzyme. After treatment with PNGase, almost all the cathepsin D migrated faster on the gel to the same position as that observed with the wild-type lysate. These findings show that most of the cathepsin D of the *GNPTAB*$^{-/-}$ mice contains two complex-type glycans, whereas a minority of the molecules contains one high-mannose and one complex-type glycan. This difference in processing of the two N-linked glycans of cathepsin D reflects the fact that the presence of Man-6-P residues on high-mannose glycans prevents processing to com-

TABLE 2. Lysosomal Enzyme Activities in Eye Lysates

Enzymes	GNPTAB Wild-Type (+/+)	GNPTAB Homozygote (−/−)	GNPTAB Heterozygote (+/−)
β-Hexosaminidase	17.0	25.0	17.8
α-Mannosidase	8.1	17.4	9.9
β-Mannosidase	5.9	9.2	8.0
β-Galactosidase	7.3	7.4	9.0
β-Glucuronidase	11.8	16.3	12.3

Enzyme activity is expressed in nanomoles per milligram per hour. The eyes of three mice from each genotype were combined, homogenized in buffer, and assayed for enzymatic activity. The data represent the average of two separate determinations, each performed in duplicate.

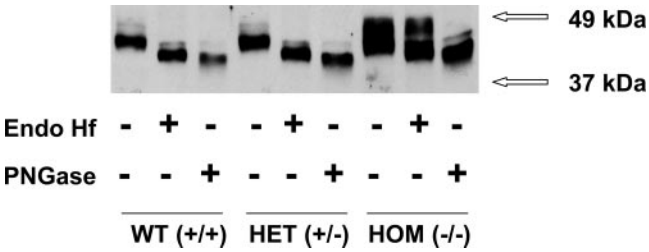

FIGURE 6. Immunoblot analysis of cathepsin D in eye lysates from wild-type (+/+), heterozygous (+/−), and homozygous (−/−) *GNPTAB*-deficient mice. Aliquots of the lysates were treated with Endo H or PNGase before SDS-PAGE.

plex-type species. In the wild-type and heterozygous samples, the glycans would be expected to be mostly phosphorylated high-mannose units.[26] In the absence of GlcNAc-1-phosphotransferase activity as occurs in the mice lacking *GNPTAB*, these glycans are processed to complex-type species that migrate slower in SDS-PAGE.

Discussion

ML II in humans (also known as I-cell or inclusion-cell disease) is characterized by coarse facial features, severe skeletal abnormalities, and psychomotor retardation. Birth weight and length are often below normal, and the diagnosis is usually made at birth or shortly afterward. The clinical course is characterized by progressive failure to thrive and developmental delay, with death occurring during the first decade.[1]

A characteristic feature of ML II is the presence of numerous membrane-bound vacuoles in the cytoplasm of mesenchymal cells, especially fibroblasts. These represent inclusion bodies that gave rise to the name I-cell disease. The skeletal system is severely affected, and abnormalities of cartilage structure are present. Serum lysosomal enzyme levels are greatly increased, secondary to faulty targeting of these enzymes to lysosomes. The cat model of ML II shows many of these manifestations but differs in the development of diffuse retinal degeneration, leading to blindness by 4 months of age. ML II has been demonstrated to result from mutations in *GNPTAB* that are inherited in an autosomal recessive manner.[3–7,9]

Phenotypic analysis of mice lacking the *GNPTAB* gene showed some similarities to human and cat ML II as well as considerable differences. Overall, the phenotype observed in *GNPTAB*$^{-/-}$ mice is not as deleterious as that in humans. The knockout mice exhibited growth retardation and a decrease in body weight, but also exhibited relatively normal life spans. Biochemically, the serum lysosomal enzyme levels were greatly increased, similar to that observed in humans and affected cats. Fibroblasts obtained from mice deficient in *GNPTAB* did not show the typical inclusion bodies that are characteristic of ML II. However, analysis of a variety of tissues revealed the widespread involvement of secretory cells in several exocrine glands, most notably in pancreas acinar cells and parotid salivary glands, similar to pathologic changes described in secretory cells of exocrine glands of several infants with ML II.[27]

Perhaps the most striking manifestation of *GNPTAB*-knockout mice was the development of a relatively late-onset retinal degeneration that resembles the retinopathy reported in the feline ML II model. Although similar retinal lesions have not been reported in humans with ML II, it is possible that the relatively long lifespan of *GNPTAB*$^{-/-}$ mice compared with affected humans might allow enough time for these age-related lesions to develop in mice, but not in infants or young children. Certainly, there are many age-related retinopathies in which cumulative effects eventually manifest in rapid-onset retinal degeneration. However, the presence of retinal lesions in young kittens with ML II suggests that species-dependent differences in lysosomal enzyme levels or requirements may be more important than age in the pathogenesis of the retinopathy. The absence of retinal lesions in aged ML III mice, which retain low levels of residual GlcNAc-1-phosphotransferase activity, suggests that a low, critical threshold level of phosphorylated lysosomal enzyme synthesis in the retina is sufficient to prevent onset of photoreceptor degeneration (Vogel P, unpublished data, 2005).[28]

Another puzzling aspect of the development of retinal degeneration in the *GNPTAB*$^{-/-}$ mice was the finding of normal levels of activity of five acid hydrolases measured in total eye extracts. However it should be noted that these extracts are derived from the vitreous fluid as well as multiple cell types. Therefore it will require additional studies to determine whether all the cell types have normal levels of these enzymes, whether the enzymes are properly localized to lysosomes, or whether other acid hydrolases not measured might be deficient.

An additional notable alteration in the *GNPTAB*-knockout mouse was the marked vacuolization of the exocrine glands, with the most severe lesions being in the pancreatic and salivary gland acinar cells. Although the basis for these alterations remains to be elucidated, it should be noted that the Man-6-P targeting pathway has been implicated in the maturation of secretory granules as they form in the trans-Golgi network.[29] Thus, it has been reported that newly formed secretory granules contain considerable amounts of lysosomal enzymes that are subsequently removed by the Man-6-P receptors which are incorporated into AP-1-containing, clathrin-coated vesicles that bud from the maturing secretory granules. In the *GNPTAB*-knockout mice, the lysosomal enzymes would lack the Man-6-P residues required for binding to the Man-6-P receptors. Consequently, these hydrolases would remain with the secretory granules where they could damage the contents, perhaps leading to the abnormal morphology that was observed. We plan to examine this possibility in our future studies.

It has been reported that the level of some lysosomal enzymes in the liver, spleen, kidneys, and brain of patients with ML II are normal or close to normal.[30,31] Our finding of normal levels of five acid hydrolases in the eyes of the *GNPTAB*-knockout mice is consistent with these publications. Similar findings have been published for the triple-knockout mice.[12] These authors showed that thymocytes from these animals use a Man-6-P-independent intracellular targeting system, whereas hepatocytes secrete their newly synthesized lysosomal enzymes and subsequently recapture them from the media. The existence of a Man-6-P-independent intracellular pathway has also been demonstrated in lymphoblasts from patients with ML II.[32] The molecular components of the Man-6-P-independent intracellular targeting system have not been defined. Nor is it known how much this capacity varies among tissue types and species. More is known about the mechanisms for recapturing lysosomal enzymes that have been released into the extracellular spaces. In addition to the carbohydrate-specific endocytic receptors present on the surfaces of selected cell types, it has recently been reported that megalin on the apical surface of kidney proximal tubular cells binds and internalizes the lysosomal enzyme cathepsin B via a noncarbohydrate mechanism.[33] Similarly, the low-density lipoprotein-related protein has been implicated in the uptake and lysosomal delivery of saposins, the activators of lysosomal sphingolipid degeneration.[34] Differences in these alternative targeting pathways could account for the phenotypic variations observed between humans, cats, and mice lacking the α,β subunits of GlcNAc-1-phosphotransferase. Studies measuring the lysosomal enzyme content of tissue from the *GNPTAB*$^{-/-}$ mice are in progress.

Although the *GNPTAB*-knockout mouse does not provide an exact mimic of the human disease, its less severe phenotype will enable studies designed to understand alternative molecular mechanisms involved in the trafficking of lysosomal enzymes to lysosomes. This mouse model should also provide a valuable tool for probing the role of proper lysosome function in the maintenance of the retina and the secretory cells of exocrine glands.

Acknowledgments

The authors thank Bobby Joe Payne, Mary Thiel, Holly Jones, and Carol Jones for technical assistance.

References

1. Kornfeld S, Sly WS. I-cell disease and pseudo-hurler polydystrophy: disorders of lysosomal enzyme phosphorylation and localization. In: Scriver CR, Beaudet AL, Sly WS, Valle D, eds. *The Metabolic and Molecular Basis of Inherited Disease*. New York: McGraw-Hill Professional; 2000;3469–3482.
2. Bao M, Elmendorf BJ, Booth JL, Drake RR, Canfield WM. Bovine UDP-*N*-acetylglucosamine:lysosomal-enzyme *N*-Acetylglucosamine-1-phosphotransferase. II. Enzymatic characterization and identification of the catalytic subunit. *J Biol Chem*. 1996;271:31446–31451.
3. Raas-Rothschild A, Cormier-Daire V, Bao M, et al. Molecular basis of variant pseudo-Hurler polydystrophy (mucolipidosis IIIC). *J Clin Invest*. 2000;105:673–681.
4. Paik KH, Song SM, Ki CS, et al. Identification of mutations in the GNPTA (MGC4170) gene coding for GlcNAc-phosphotransferase alpha/beta subunits in Korean patients with mucolipidosis type II or type IIIA. *Hum Mutat*. 2005;26:308–314.
5. Bargal R, Zeigler M, Abu-Libdeh B, et al. When mucolipidosis III meets mucolipidosis II: GNPTA gene mutations in 24 patients. *Mol Genet Metab*. 2006;88:359–363.
6. Raas-Rothschild A, Bargal R, Goldman O, et al. Genomic organisation of the UDP-*N*-acetylglucosamine-1-phosphotransferase gamma subunit (GNPTAG) and its mutations in mucolipidosis III. *J Med Genet*. 2004;41:52–56.
7. Kudo M, Brem MS, Canfield WM. Mucolipidosis II (I-cell disease) and mucolipidosis IIIA (classical pseudo-hurler polydystrophy) are caused by mutations in the GlcNAc-phosphotransferase alpha/beta-subunits precursor gene. *Am J Human Genet*. 2006;78:451–463.
8. Kudo M, Bao M, D'Souza A, et al. The α- and β-subunits of the human UDP-*N*-acetylglucosamine:lysosomal enzyme phosphotransferase are encoded by a single cDNA. *J Biol Chem*. 2005;280:36141–36149.
9. Tiede S, Storch S, Lubke T, et al. Mucolipidosis II is caused by mutations in GNPTA encoding the α/β GlcNAc-1-phosphotransferase. *Nat Med*. 2005;11:1109–1112.
10. Mazrier H, Van Hoeven M, Wang P, et al. Inheritance, biochemical abnormalities, and clinical features of feline mucolipidosis II: the first animal model of human I-cell disease. *J Hered*. 2003;94:363–373.
11. Dittmer F, Hafner A, Ulbrich EJ, et al. I-cell disease-like phenotype in mice deficient in mannose 6-phosphate receptors. *Transgenic Res*. 1998;7:473–483.
12. Dittmer F, Ulbrich EJ, Hafner A, et al. Alternative mechanisms for trafficking of lysosomal enzymes in mannose 6-phosphate receptor-deficient mice are cell type-specific. *J Cell Sci*. 1999;112:1591–1597.
13. Zambrowicz BP, Abuin A, Ramirez-Solis R, et al. Wnk1 kinase deficiency lowers blood pressure in mice: a gene-trap screen to identify potential targets for therapeutic intervention. *Proc Natl Acad Sci*. 2003;100:14109–14114.
14. Zambrowicz BP, Friedrich GA, Buxton EC, Lilleberg SL, Person C, Sands AT. Disruption and sequence identification of 2,000 genes in mouse embryonic stem cells. *Nature*. 1998;392:608–611.
15. Joyner AL. *Gene Targeting: A Practical Approach*. Oxford, UK: Oxford University Press; 2000.
16. Silver J, Keerikatte V. Novel use of polymerase chain reaction to amplify cellular DNA adjacent to an integrated provirus. *J Virol*. 1989;63:1924–1928.
17. Rice DS, Huang W, Jones HA, et al. Severe retinal degeneration associated with disruption of semaphorin 4A. *Invest Ophthalmol Vis Sci*. 2004;45:2767–2777.
18. Schrick J, Vogel P, Abuin A, Hampton B, Rice D. ADP-ribosylation factor-like 3 is involved in kidney and photoreceptor development. *Am J Pathol*. 2006;168:1288–1298.
19. Simmons DM, Arriza JL, Swanson LW. A complete protocol for *in situ* hybridization of messenger RNAs in brain and other tissues with radiolabeled single-stranded RNA probes. *J Histotech*. 1989;12:169–181.
20. Varki A, Reitman ML, Vannier A, Kornfeld S, Grubb JH, Sly WS. Demonstration of the heterozygous state for I-cell disease and pseudo-Hurler polydystrophy by assay of N-acetylglucosaminylphosphotransferase in white blood cells and fibroblasts. *Am J Hum Genet*. 1982;34:717–729.
21. Beltrandelrio H, Kern F, Lanthorn TH, et al. Saturation screening of the druggable mammalian genome. In: Carroll PM, Fitzgerald K, eds. *Model Organisms in Drug Discovery.* Chichester, UK; John Wiley & Sons; 2003;251–279.
22. Hanai J, Leroy J, O'Brien JS. Ultrastructure of cultured fibroblasts in I-cell disease. *Am J Dis Child*. 1971;122:34–38.
23. Leroy JG, Spranger JW, Feingold M, Opitz JM, Crocker AC. I-cell disease: a clinical picture. *J Pediatr*. 1971;79:360–365.
24. Traboulsi EI, Maumenee IH. Ophthalmologic findings in mucolipidosis III (pseudo-Hurler polydystrophy). *Am J Ophthalmol*. 1986;102:592–597.
25. Koike M, Shibata M, Ohsawa Y, et al. Involvement of two different cell death pathways in retinal atrophy of cathepsin D-deficient mice. *Mol Cell Neurosci*. 2003;22:146–161.
26. Dittmer F, Pohlmann R, von Figura K. The phosphorylation pattern of oligosaccharides in secreted procathepsin D is glycosylation site-specific and independent of the expression of mannose 6-phosphate receptors. *J Biol Chem*. 1997;272:852–858.
27. Elleder M, Martin JJ. Mucolipidosis type II with evidence of a novel storage site. *Virchows Arch*. 1988;433:575–578.
28. Lee WS, Payne BJ, Gelfman CM, Vogel P, Kornfeld S. Murine UDP-GlcNAc:lysosomal enzyme N-acetylglucosamine-1-phosphotransferase lacking the gamma subunit retains substantial activity toward acid hydrolases. *J Biol Chem*. In press.
29. Klumperman J, Kuliawat R, Griffith J, Geuze H, Arvan P. Mannose 6-phosphate receptors are sorted from immature secretory granules via adaptor protein AP- 1, clathrin, and syntaxin 6-positive vesicles. *J Cell Biol*. 1998;141:359–371.
30. Waheed A, Pohlmann R, Hasilik A, von Figura K, van Elsen A, Leroy G. Deficiency of UDP-N-acetylglucosamine: lysosomal enzyme N-acetylglucosamine-1-phosphotransferase in organs of I-cell patients. *Biochem Biophys Res Commun*. 1982;105:1052–1058.
31. Owada M, Neufeld E. Is there a mechanism for introducing acid hydrolases into liver lysosomes that is independent of mannose 6-phosphate recognition?—evidence from I-cell disease. *Biochem Biophys Res Commun*. 1982;105:814–820.
32. Glickman J, Kornfeld S. Mannose 6-phosphate-independent targeting of lysosomal enzymes in I-cell disease B lymphoblasts. *J Cell Biol*. 1993;123:99–108.
33. Nielsen R, Courtoy P, Jacobsen C, et al. Endocytosis provides a major alternative pathway for lysosomal biogenesis in kidney proximal tubular cells. *Proc Natl Acad Sci USA*. 2007;104:5407–5412.
34. Hiesberger T, Hüttler S, Rohlmann A, Schneider W, Sandhoff K, Herz J. Cellular uptake of saposin (SAP) precursor and lysosomal delivery by the low density lipoprotein receptor-related protein (LRP). *EMBO J*. 1998;17:4617–4625.